56th LPSC (2025) 1391.pdf

ROUGHNESS DISTRIBUTION IN THE EQUATORIAL REGION OF MERCURY.

G. Nishiyama^{1,2,3}, F. Preusker¹, A. Broquet¹, A. Stark¹, H. Hussmann¹, ¹Institute for Planetary Research, DLR, Germany, (gaku.nishiyama@dlr.de), ²Department of Earth and Planetary Science, The University of Tokyo, ³National Astronomical Observatory of Japan

Introduction: Topographic roughness is a useful tool for studying surface evolution on rocky planets. Roughness on Mercury has been investigated using data from the Mercury Laser Altimeter (MLA) onboard Space Environment, Geochemistry, and Ranging (MESSENGER) mission [1]. MLA has successfully mapped roughness on Mercury at baselines down to sub-km scales [2, 3, 4, 5], though its observation is limited to the north-polar region because of the eccentric orbit of MESSENGER and the limited ranging distance of MLA.

One way to complement the lack of roughness data in the equatorial region is to use image-based digital elevation models (DEMs). The MESSENGER Global DEM MSGR_DEM_USG_SC_I_V02 [6] has been used to quantify roughness on a global scale [7]. However, a previous study reported that this DEM does not resolve topography at km scale because of interpolation and over-smoothing during the DEM production [7]. Therefore, roughness map at km-scale baselines is still missing for the region below 45°N latitude on Mercury.

In this study, we present a new roughness map in the equatorial region of Mercury based on the latest global DEM (version 20240927) produced as described in Preusker et al. [8]. Comparison between the DEM and images has shown that the effective resolution of this DEM is approximately 5 km [8, 9]. Investigating roughness with this DEM, we present anomalous features in roughness at the kilometric scale and discuss the correlation between roughness distribution and other geologic features.

Method: As an indicator of roughness, we focus on topographic curvatures as in previous studies [4, 10]. Unlike other roughness measures such as RMS deviation, the curvature of topography is not sensitive to large-scale tilts of the surface and can reflect convex and concave surfaces. First, we calculated the curvature values at each DEM grid element by comparing surface heights at other points separated by a certain distance. To statistically examine roughness distribution, the difference between 75 % and 25 % quantiles of curvature values was calculated at each location and used to map roughness distribution as surface curvature variability.

The median curvature normalized by the interquartile ranges was also used to characterize roughness, which we argue to be representative of surface age. Because craters exhibit concave topography except for their rims, heavily cratered terrain on airless bodies typically shows positive concavity [e.g., 10]. However, fresh surfaces, such as young basin ejecta, typically show less concave topographies.

Results and implications: Figure 1 shows the roughness distribution as an RGB-composite map. In this RGB composite map, the interquartile ranges at baselines of 5 km and 10 km are used for the red and green channels. The normalized median of curvatures at a 10-km baseline is plotted in the blue channel. Therefore, smoother locations appear darker in the RGB map.

The most obvious feature in the RGB map is the boundary between the smooth and intercrater plains. Similar to previous works for the northern hemisphere

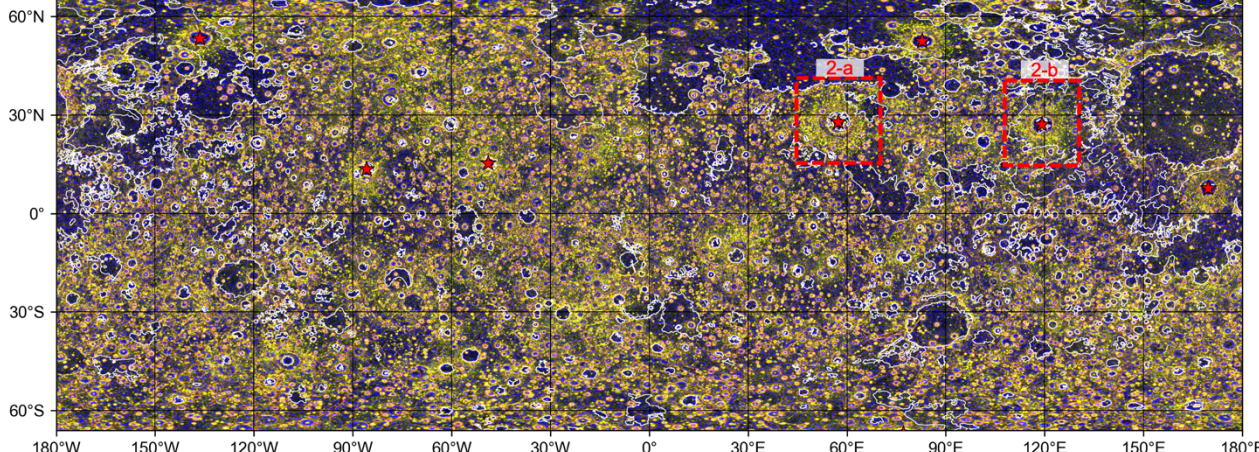


Figure 1. The RGB-composite roughness map in a cylindrical projection. The red stars show locations of craters that have diameters larger than 150 km and degradation class of 4 (i.e., fresh) [11]. The white lines denote outlines of the smooth plains [14].

56th LPSC (2025) 1391.pdf

[4], the interquartile range in the dark smooth plains is half of that in bright intercrater plains on average. However, the roughness is not uniform over all the smooth plains. For example, the Caloris smooth plains show higher roughness than the northern smooth plains. This variation originates from grabens inside Caloris whose widths reach a few kilometers [e.g., 12].

Figure 1 also shows bright roughness anomalies around young basins (stars in Figure 1), implying a decrease in roughness with age. Figures 2-a and b show maps of interquartile ranges at two basins: Rachmaninoff and Raditladi. The areas of continuous ejecta have higher roughness and less concavity than the surroundings due to their freshness. The roughness distributions inside the continuous ejecta have local minima adjacent to the rim (indicated by the white arrow in Figure 2-c), similar to craters in the northern hemisphere [2]. This feature is commonly found at young basins (Figure 1), suggesting coverage of impact melt and/or paucity of secondary craters within 30–50 % of the radius from the crater rim.

A further characteristic at the roughness anomalies is the absence of contractional landforms. Based on the latest catalog [13], the contractional landforms are not mapped inside the rough areas of continuous ejecta (Figure 2). The analysis of the roughness map indicates the existence of this tendency over the whole equatorial

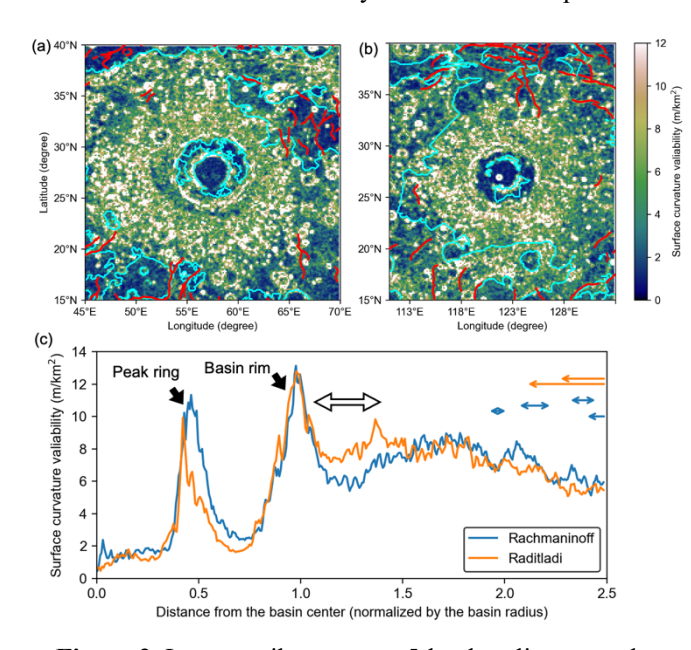


Figure 2. Interquartile ranges at 5-km baseline around two basins. (a) Rachmaninoff. (b) Raditladi. The red line shows locations of contractional landforms [13]. The cyan lines show outlines of smooth plains [14]. (c) The azimuthal average of interquartile range as a function of distance from the basin centers. The orange and blue arrows show locations of contraction features [13].

region. Figure 3 presents histograms of interquartile ranges in intercrater plains. While ridges and scarps contribute to an increase in roughness, roughness at such contractional landforms is lower than the average. This correlation may suggest three possibilities. First, ejecta deposition from younger basins may mask older tectonic features. Second, roughness may make it difficult to detect tectonic landforms by visual inspection. Third, contractional landforms could be less likely to form in rough regions. Heavily-cratered (i.e., rough) terrains may have high crustal porosity [15], which makes local crustal material less competent for fault formations. If one of them is the case, previous studies may have underestimated the extent of the Mercury's radial contraction due to the obscuration of old contractional landforms. Further work on the correlation between roughness and tectonics may provide insights into the extent to which corrections to global contraction estimates are necessary to account for the roughness effect.

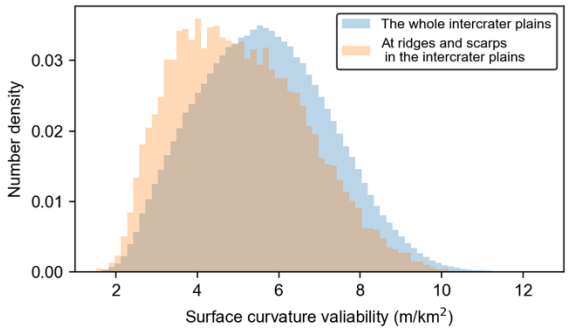


Figure 3. Histograms of interquartile ranges at 5-km baselines in the intercrater plains.

Acknowledgments: This work was supported by JSPS KAKENHI Grant Number JP22K21344 and JSPS Overseas Research Fellowship.

References: [1] Zuber M. T. et al. (2012) Science, 336, 217–220. [2] Susorney H. C. M. et al. (2017) JGR: *Planets*, 123, 1581–1595. [3] Pommerol A. et al. (2012) Planetary and Space Science, 73, 287–293. [4] Kreslavsky M. A. et al. (2014) GRL, 41, 8245-8251. [5] Fa W. (2016) GRL, 43, 3078-3087. [6] Becker K. J. et al. (2016) 47th LPSC, Abstracts #2959.[7] Florinsky I. V. (2018) Planetary and Space Science, 151, 56-70. [8] Preusker F. et al. (2017) Planetary and Space Science, 142, 26-37. [9] Stark A. et al. (2015) Planetary and Space Science, 117, 64-72. [10] Kreslavsky M. A. & Head J. W. (2012) JGR: Planets, 117, E00H24. [11] Kinczyk M. J. et al. (2020) Icarus, 341, 113637. [12] Murchie S. L. et al. (2008) *Science*, 321, 73–76. [13] Klimczak C. et al. (2023) 54th LPSC, Abstract #1122. [14] Denevi B. W. et al. (2013) JGR: Planets, 118, 891-907. [15] Broquet A. et al. (2024) GRL, e2024GL110583.